

**AD-A249 010**



WL-TR-91-2094

OPTICAL AND ELECTRICAL CHARACTERISTICS OF THE  
CATHODE FALL

Z. Lj. PETROVIĆ and A. V. PHELPS

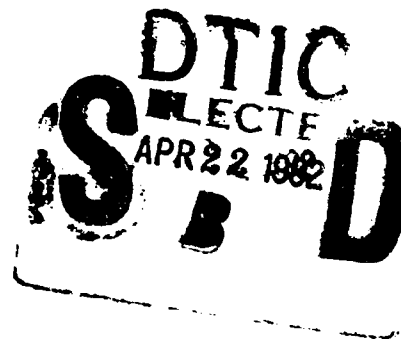
JOINT INSTITUTE FOR LABORATORY ASTROPHYSICS  
QUANTUM PHYSICS DIVISION  
NATIONAL INSTITUTE OF STANDARDS AND TECHNOLOGY  
BOULDER, CO 80303

January 1992

FINAL REPORT FOR PERIOD OCTOBER 1989 - SEPTEMBER 1990

Approved for public release; distribution is unlimited

AERO PROPULSION AND POWER DIRECTORATE  
WRIGHT LABORATORY  
AIR FORCE SYSTEMS COMMAND  
WRIGHT-PATTERSON AIR FORCE BASE, OHIO 45433-6563



**92-10015**

92 4 20 037

## NOTICE

When Government drawings, specifications, or other data are used for any purpose other than in connection with a definitely Government-related procurement, the United States Government incurs no responsibility or any obligation whatsoever. The fact that the Government may have formulated or in any way supplied the said drawings, specifications, or other data, is not to be regarded by implication, or otherwise in any manner construed, as licensing the holder, or any other person or corporation to manufacture, use, or sell any patented invention that may in any way be related thereto.

This report is releasable to the National Technical Information Service (NTIS). At NTIS, it will be available to the general public, including foreign nations.

This technical report has been reviewed and is approved for publication.



Monitor

Research Physicist  
Advanced Plasma Research Group  
Power Components Branch  
Aerospace Power Division  
Aero Propulsion and Power Directorate



Supervisor

LOWELL D. MASSIE  
Chief, Power Components Branch  
Aerospace Power Division  
Aero Propulsion and Power Directorate



for Div. Chief  
WILLIAM U. BORGER  
Chief, Aerospace Power Division  
Aero Propulsion & Power Directorate

If your address has changed, if you wish to be removed from our mailing list, or if the addressee is no longer employed by your organization please notify WL/POOC, Wright-Patterson AFB, OH 45433-6563 to help us maintain a current mailing list.

Copies of this report should not be returned unless return is required by security considerations, contractual obligations, or notice on a specific document.

UNCLASSIFIED

SECURITY CLASSIFICATION OF THIS PAGE

## REPORT DOCUMENTATION PAGE

Form Approved  
OMB No. 0704-0188

1a. REPORT SECURITY CLASSIFICATION Unclassified			1b. RESTRICTIVE MARKINGS		
2a. SECURITY CLASSIFICATION AUTHORITY			3. DISTRIBUTION / AVAILABILITY OF REPORT Approved for public release; distribution is unlimited		
2b. DECLASSIFICATION / DOWNGRADING SCHEDULE					
4. PERFORMING ORGANIZATION REPORT NUMBER(S)			5. MONITORING ORGANIZATION REPORT NUMBER(S) WL-TR-91-2094		
6a. NAME OF PERFORMING ORGANIZATION Quantum Physics Division National Inst. of Standards & Technology		6b. OFFICE SYMBOL (if applicable)	7a. NAME OF MONITORING ORGANIZATION Wright Lab., Aero Propulsion & Power Dir. (WL/POOC)		
6c. ADDRESS (City, State, and ZIP Code) Boulder, CO 80303			7b. ADDRESS (City, State, and ZIP Code) Wright-Patterson AFB, OH 45433-6563		
8a. NAME OF FUNDING / SPONSORING ORGANIZATION Wright Research and Development Center		8b. OFFICE SYMBOL (if applicable) WL-POOC	9. PROCUREMENT INSTRUMENT IDENTIFICATION NUMBER MIPR 90-C-0867		
8c. ADDRESS (City, State, and ZIP Code) Aero Propulsion & Power Lab. (WRDC/POOC-3) Wright-Patterson AFB, OH 45433-6563			10. SOURCE OF FUNDING NUMBERS		
			PROGRAM ELEMENT NO. 61102F	PROJECT NO. 2301	TASK NO. S1
					WORK UNIT ACCESSION NO. 24
11. TITLE (Include Security Classification) Optical and Electrical Characteristics of the Cathode Fall					
12. PERSONAL AUTHOR(S) Z. Lj. Petrovic and A. V. Phelps					
13a. TYPE OF REPORT Final		13b. TIME COVERED FROM Oct. 89 TO Sept. 90		14. DATE OF REPORT (Year, Month, Day) 1992 January	
15. PAGE COUNT 30					
16. SUPPLEMENTARY NOTATION					
17. COSATI CODES			18. SUBJECT TERMS (Continue on reverse if necessary and identify by block number)		
FIELD	GROUP	SUB-GROUP	Hydrogen, nitrogen, argon, cathode fall, discharge, voltage-current, oscillation, constriction, absorption, charge multiplication, inductance, damping		
20	6	19			
20	9	4			
19. ABSTRACT (Continue on reverse if necessary and identify by block number) Experiments with hydrogen discharges dominated by the cathode fall show that a) these discharges are unstable for wide ranges of current and circuit resistance, b) increasing the circuit capacitance expanded the region of instabilities to lower currents, c) lateral constrictions of the discharge occur over a much more limited range of currents and pressures than do oscillations, d) laser-induced photoelectron pulses produce damped oscillations for discharge currents below those at which self-sustained oscillations are observed, e) the frequency of the induced oscillations varies approximately as the square root of the discharge current, and f) the damping of the oscillations increases with discharge current in an as yet unexplained manner. Measurements of the electronic charge multiplication at voltages below and above the breakdown or low-current-maintenance voltage showed an unexpected discontinuity at the breakdown voltage.					
20. DISTRIBUTION / AVAILABILITY OF ABSTRACT <input checked="" type="checkbox"/> UNCLASSIFIED/UNLIMITED <input type="checkbox"/> SAME AS RPT. <input type="checkbox"/> DTIC USERS			21. ABSTRACT SECURITY CLASSIFICATION Unclassified		
22a. NAME OF RESPONSIBLE INDIVIDUAL A. Garscadden			22b. TELEPHONE (Include Area Code) (513)255-2923		22c. OFFICE SYMBOL WL/POOC

## PREFACE AND ACKNOWLEDGMENTS

This work was performed by the Quantum Physics Division, National Institute of Standards and Technology, at the Joint Institute for Laboratory Astrophysics under MIPR FY1455-89-N0665 and FY1455-90-N0625. The work was performed during the period October 1989 through September 1990 under Project 2301 Task S1, Work Unit 24. The Air Force contract manager was Dr. Alan Garscadden, Energy Conversion Branch, Wright Laboratory, WPAFB, OH 45433-6563.

We would like to acknowledge suggestions from A. Gallagher regarding the experiments and their interpretation and the help of J. D. Krakover, R. A. Mitchell and J. Fenney with the computer. The work was supported in part by the National Institute of Standards and Technology.

<b>Accession For</b>	
NTIS GRA&I	<input checked="" type="checkbox"/>
DTIC TAB	<input type="checkbox"/>
Unannounced	<input type="checkbox"/>
Justification	
By	
Distribution/	
Availability Codes	
Dist	Avail and/or Special
A-1	



## TABLE OF CONTENTS

SECTION	PAGE
I. INTRODUCTION . . . . .	1
II. EXPERIMENTAL TECHNIQUE . . . . .	4
III. VOLTAGE-CURRENT MEASUREMENTS . . . . .	7
IV. STABILITY CHARACTERISTICS . . . . .	10
V. DISCHARGE CONSTRICTIONS . . . . .	12
VI. SEARCH FOR ABSORPTION BY $N_2^+$ . . . . .	13
VII. ELECTRONIC CHARGE MULTIPLICATION . . . . .	15
VIII. LASER-INDUCED DISCHARGE OSCILLATION . . . . .	18
IX. CONCLUSIONS AND RECOMMENDATIONS . . . . .	22
REFERENCES . . . . .	24

## LIST OF ILLUSTRATIONS

FIGURE		PAGE
1.	Schematic of discharge tube. . . . .	5
2.	Schematic of electrical circuit . . . . .	6
3.	Discharge characteristics for $H_2$ at 0.5 Torr. (a) Voltage-current data. (b) Stability diagram. . . . .	8
4.	Discharge characteristics for $H_2$ at 3 Torr. (a) Voltage-current data. (b) Stability diagram. . . . .	9
5.	Electron charge ratios $Q_e/Q_c$ for Ar at $E/n = 1$ kTd. . . . .	16
6.	Photoelectron induced transient current waveforms in $H_2$ for a $pd = 0.55$ Torr cm. . . . .	19
7.	Angular frequency and damping constant versus current for $pd = 0.55$ Torr cm. . . . .	21

## SECTION I

### INTRODUCTION

This report summarizes results obtained under the project entitled "Optical and Electrical Characteristics of the Cathode Fall" for the period from 1 October 1989 to 30 September 1990. It is submitted by the Quantum Physics Division of the National Institute of Standards and Technology to the Air Force Wright Laboratory. The research was carried out at the Joint Institute for Laboratory Astrophysics with the direct supervision and participation of Dr. A.V. Phelps, Principal Investigator.

The objective of this research is to extend and apply experimental diagnostics and simple models to the optical and electrical behavior of the cathode fall regions of electrical discharges in gases that are of interest to the Air Force. Since the beginning of this project in October 1989 we have a) designed, constructed, and tested a parallel plane electrode discharge tube suitable for operation at the high current densities representative of practical cathode-fall dominated discharges; b) measured voltage-current characteristics over a wide range of currents and pressures; c) determined the range of currents as a function of the external resistance and pressure for which the discharge can operate and for which it is free of oscillations; d) determined the range of currents as a function of external resistance and pressures for which the discharge is constricted; e) made exploratory measurements of the electronic charge multiplication when a laser-induced photoelectron pulse is superimposed on a dc discharge; and f) made measurements of the frequency and damping of transient oscillations of the discharge current resulting from the release of a pulse of photoelectrons from the cathode. The measurements of discharge operating conditions have been carried out in  $H_2$ ,  $N_2$ , and Ar,

although the greatest emphasis in the analysis has been on  $H_2$  because of the greater current Air Force interest in  $H_2$ .

Pulsed electrical discharges in molecular gases, such as  $H_2$ , are of interest to the Air Force because of their use in devices such as high power switches, electrically excited lasers, and plasma processors. Because of their role in natural phenomena such as lightning and corona, it is important that one be able to predict the contribution of multistep processes to the growth of ionization in molecular gases such as  $N_2$ . Gas discharges play a key role in the production of semiconductors. An important aspect of this program is the development of nonintrusive diagnostics of electrical discharges in molecular gases.

This report includes the following:

- 1) The parallel-plane electrode discharge tube suitable for operation at high current densities is described in Section II;
- 2) Measurements of voltage-current characteristics over a wide range of currents and pressures are summarized in Section III;
- 3) The determination of the range of currents as a function of the external resistance and pressure for which the discharge in  $H_2$  is free of oscillations is presented in Section IV;
- 4) The determination of the range of currents as a function of external resistance and pressures for which the discharge is constricted is briefly summarized in Section V,
- 5) The search for absorption of light by  $N_2^+$  ions in the cathode fall is summarized in Section VI.
- 5) Measurements of the differential electronic charge multiplication when a laser-induced photoelectron pulse is superimposed on a dc discharge are discussed in Section VII, and



6) Measurements of the frequency and damping of transient oscillations induced by the discharge current pulse resulting from the release of photoelectrons from the cathode are presented in Section VIII.

Recommendations for future work are given in Section IX.

## SECTION II

### EXPERIMENTAL TECHNIQUE

Figure 1 shows a schematic of the discharge tube developed for these measurements of the properties of cathode-fall dominated discharges.<sup>1-3</sup> The cathode C is made of gold plated copper and is operated at a high voltage relative to the grounded vacuum shell. The gold provides a relatively stable work function for the photoelectron pulse experiments,<sup>4</sup> while the copper base provides good thermal conductivity for the temperature rise measurements. The electrode spacing is adjustable, but is set at 10 mm for the present experiments. A thermocouple in contact with the copper cathode is used to measure the temperature of the cathode. The thermocouple TC and its meter operate at the cathode voltage. The cathode lead is covered with glass and ceramic and the cathode is surrounded with a tightly fitting quartz cylinder Q so as to prevent long-path breakdown at low pressures.<sup>5</sup> The anode A is a semitransparent film of gold deposited on a quartz window. It is 60 mm in diameter and is insulated from ground for current measurements.

A schematic of the electrical circuit is shown in Figure 2. All of the data reported were obtained with a simple electrical circuit consisting of resistance  $R_S$  in series with the discharge D and a monitor resistor between the anode and ground. The voltages were supplied from a dc, voltage-regulated supply  $V_0$ . In some of the experiments the stability characteristics of the discharge were modified by changing the capacitance shunting the discharge C. The average discharge currents were measured with an electrometer I and transferred to digitizer and personal computer for storage and analyses. Similarly, the voltages across the discharge tube are

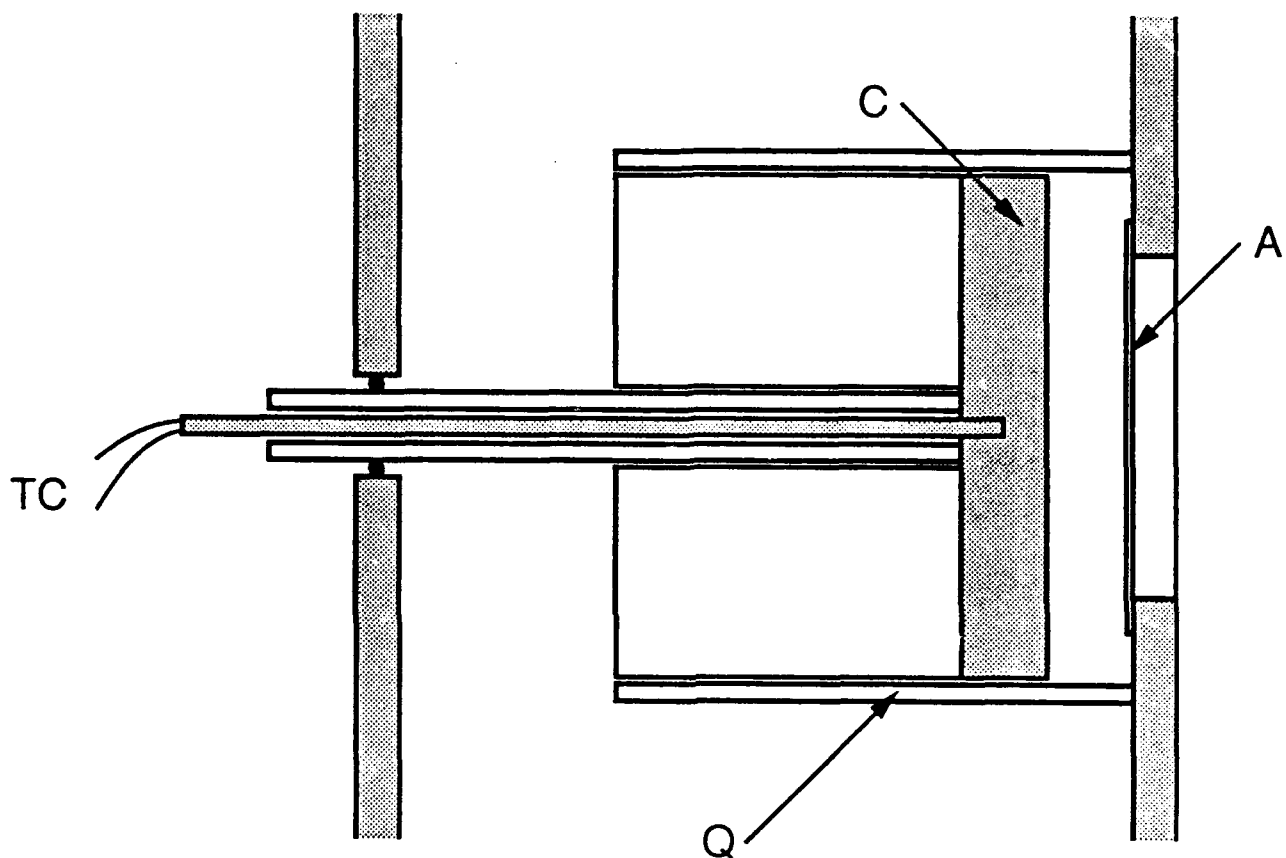


Figure 1. Schematic of discharge tube.

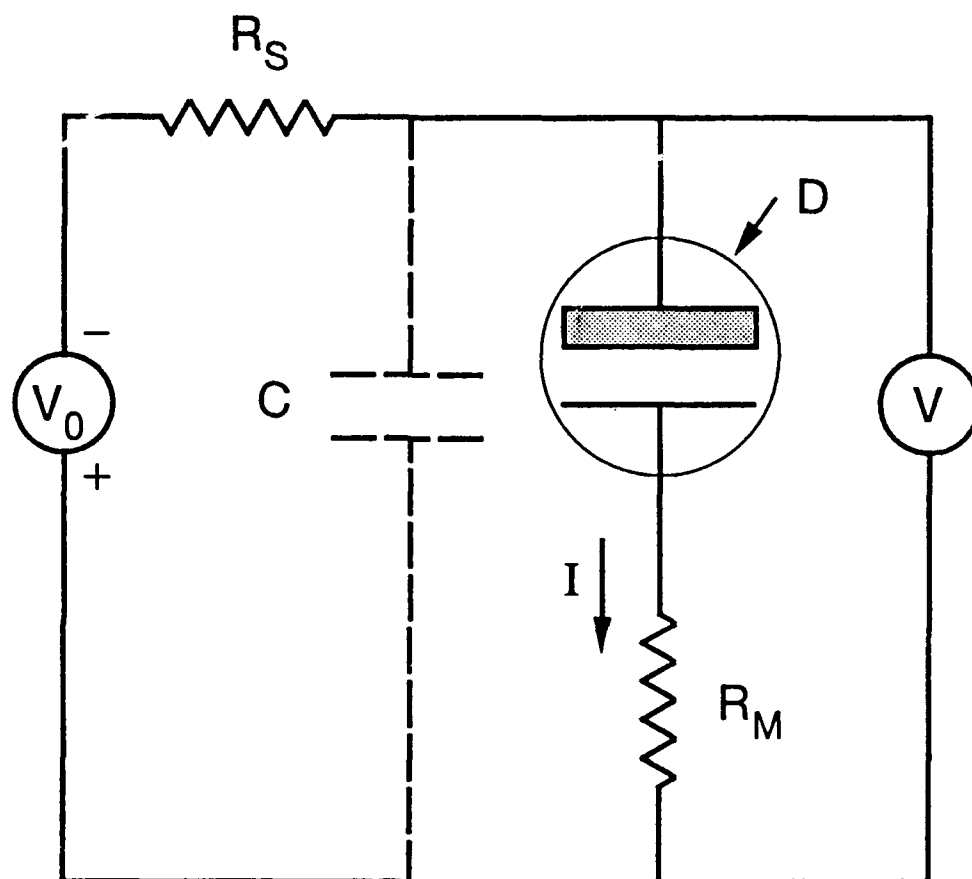


Figure 2. Schematic of electrical circuit.

measured with a high-impedance voltage divider and electrometer V and then digitized and stored in the computer. Gas pressures were measured with a diaphragm-type manometer with a stated accuracy of  $\pm 0.01$  Torr. The gas samples were taken from high pressure cylinders with a stated purity of 0.9999.

Current oscillations were detected with a wide band oscilloscope (100 MHz) and the discharge was recorded as oscillating when they reach 10% of the average current. Thus, the small amplitude ( $\approx 5\%$ ), highly-damped, high-frequency "noise" pulses observed at low currents ( $< 10^{-5}$  A) with  $H_2$  at 0.5 Torr are not designated as oscillations in this report. The transient current and voltage waveforms were initially recorded with a wide-band storage oscilloscope and then transferred to the computer.

### SECTION III

#### VOLTAGE-CURRENT MEASUREMENTS

Representative voltage-current measurements in  $H_2$  are shown in Figures 3(a) and 4(a) for pressures of 0.5 and 3 Torr, respectively. Data (not shown) were also obtained at 1 Torr. In order to obtain these data the series resistance was varied from 1 k $\Omega$  to 200 M $\Omega$ . The current range covered with each resistor was roughly a factor of 10, e.g.,  $10^{-6}$  to  $3 \times 10^{-5}$  A with series resistor of 9 M $\Omega$ . The rather large scatter for currents in the  $3 \times 10^{-3}$  to  $3 \times 10^{-2}$  A range in Figure 3(a) is related to instabilities, including oscillations, of the discharge. The same is true for discharge currents near  $10^{-3}$  A for the data of Figure 4(a).

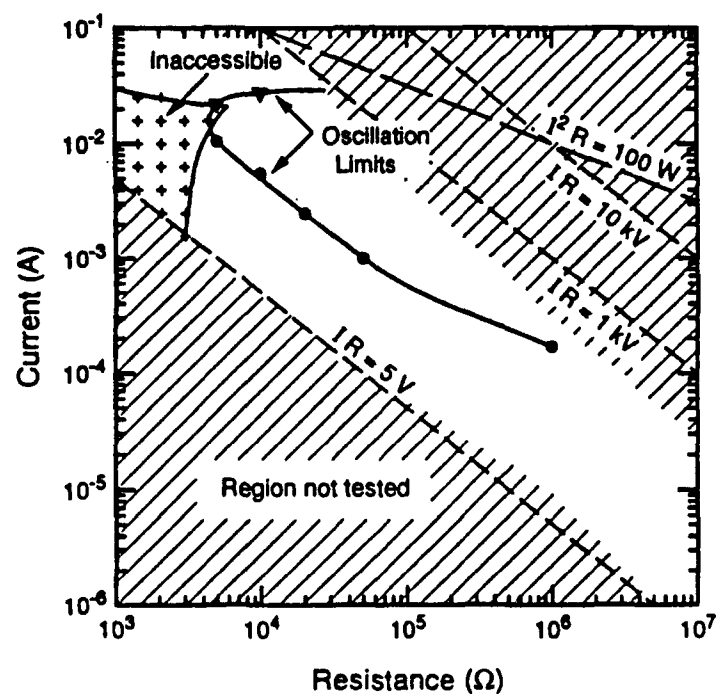
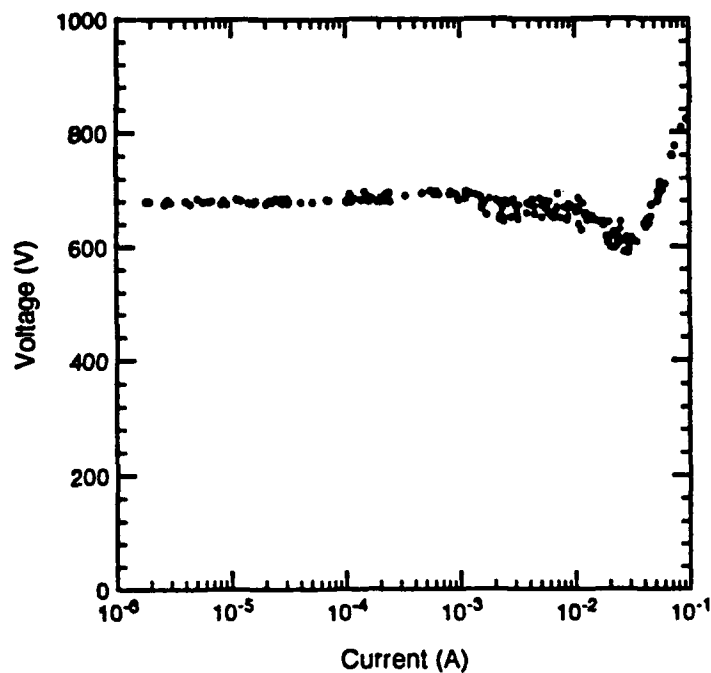
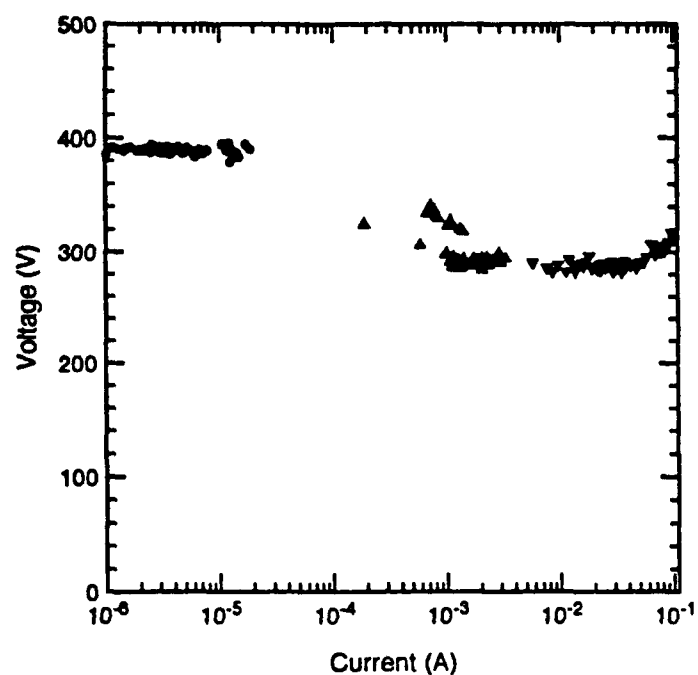
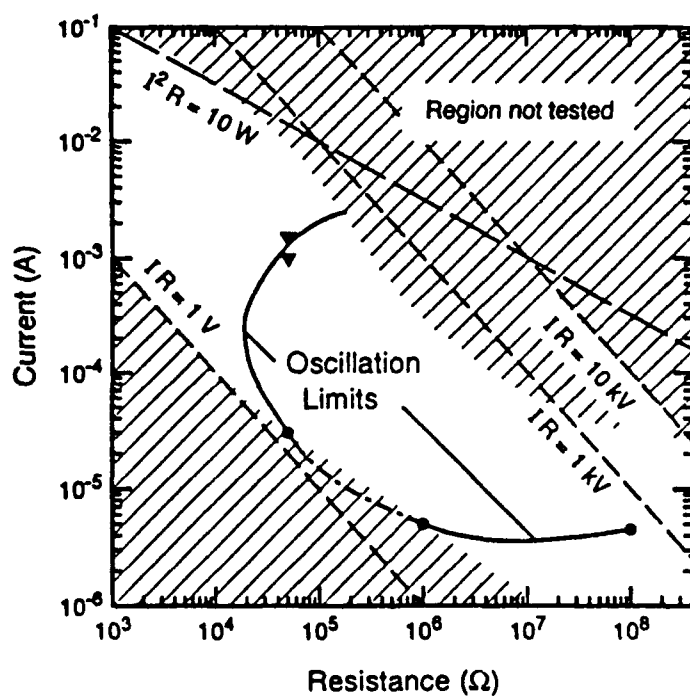


Figure 3. Discharge characteristics for  $\text{H}_2$  at 0.5 Torr. (a) Voltage-current data. (b) Stability diagram.



(a)



(b)

Figure 4. Discharge characteristics for  $H_2$  at 3 Torr. (a) Voltage-current data. (b) Stability diagram.

## SECTION IV

### STABILITY CHARACTERISTICS

Figures 3(b) and 4(b) show the stability limits for the  $H_2$  discharges for pressures of 0.5 and 3 Torr, respectively. The discharges are defined as oscillatory when the amplitude of current oscillations exceeds 10% of the average current. The limits of oscillation are indicated by the points and a smooth solid curve has been drawn through the points. Thus, the discharges oscillated "inside" the region outlined by the solid line. The form of the current oscillation is not indicated in the figures, but varies from near sinusoidal to very sharp current spikes. The shaded regions of Figures 3(b) and 4(b) were not investigated. For example, upper limits to the shaded regions at low currents and low resistances were determined by our ability to set and maintain the voltage from the power supply and by changes in the discharge voltage. These limits correspond to voltages across the series resistance ranging from 1 to 5 V and are about equal to the reproducibility and stability limits expected for the power supplies in use at that time. On the other hand, the lower limits to the shaded region at the higher currents and resistances were set by the voltages available from the power supplies and/or by the power dissipation allowable in the series resistors. The shaded regions represent areas that may be accessible with sufficient effort and do not represent known limitations set by the discharges.

In the case of discharges in  $H_2$  at 0.5 Torr, Figure 3a shows an additional region designated by crosses and labeled "inaccessible." This region is inaccessible because of the negative differential resistance behavior of the discharge in which the use of too small a series resistance results in a jump of the current over the region. The details of this behavior



have not been mapped out for the present discharges, although the general behavior is well documented in the literature.<sup>1,3</sup>

The effect of changing the circuit capacitance was measured by removing extraneous leads, e.g., the thermocouple voltmeter, and then adding known capacitances in parallel with the discharge at fixed series resistance. In general, adding capacitance expanded the region of instability to lower currents. Thus, for H<sub>2</sub> discharges at 0.5 Torr and a series resistance of 50 k $\Omega$  decreasing the measured circuit capacitance from the 500 pF of Figures 3 and 4 to the minimum of 250 pF set by the discharge tube construction raised the low current limit for oscillations from 1.5 to 2.3 mA. When the circuit capacitance was increased to 0.01  $\mu$ F the lower limit for oscillations decreased to 0.11 mA. The upper limit for oscillations was unchanged to within the uncertainty of the measurements.

It is of interest to note that experimental data showing the regions in the current-series resistance plane supporting oscillations do not appear to have been given in previous publications.<sup>1-4</sup> Theory and data needed for predicting the dependence of the lower current limit for spontaneous oscillations on circuit resistance and capacitance and on the equivalent negative resistance and inductance of the discharge have been given by Sigmond.<sup>8</sup>

For N<sub>2</sub> discharges oscillations were observed at 3 Torr with series resistances of 1 M $\Omega$  for currents between 0.22 and 0.27 mA and with 5.5 M $\Omega$  for currents between 0.26 and 0.55 mA. No oscillations were observed for pressures of 0.5 and 1 Torr. For Ar discharges oscillations were observed at 0.3 Torr with a series resistance of 1 M $\Omega$  for currents between 0.1 and 0.5 mA. No oscillations were observed for pressures of 1 and 2 Torr.

## SECTION V

### DISCHARGE CONSTRICTIONS

Records were kept of the range of discharge parameters which resulted in a visual impression of a significant spatial variation of emission from the negative glow over the area of the discharge. We will designate a discharge with such nonuniformities as a constricted negative-glow or cathode-fall discharge rather than use the conventional,<sup>1,3</sup> but uninformative, notation of a "subnormal" discharge. The case of uniform emission over the cathode surface, which is conventionally referred to as an "abnormal" glow,<sup>1,3</sup> will be called the diffuse negative glow or cathode fall. No attempt has been made to show the transition between constricted and diffuse negative-glows in Figures 3 and 4. In fact, no evidence was obtained for the existence of constricted discharges in H<sub>2</sub> at pressures of 0.5 and 1 Torr and currents from 10<sup>-6</sup> to 10<sup>-1</sup> A. At a pressure of 3 Torr of H<sub>2</sub> "constrictions", i.e., doughnut shaped brighter regions near the quartz cylinder, were observed with resistances of 1 and 50 k $\Omega$  and currents of the order of 10 mA. Although constrictions were not detected visually with the higher resistances, the small magnitude of the associated currents severely limits the observation of any emission.

Constrictions were observed with Ar discharges for pressures of 1 and 2 Torr and currents from  $3 \times 10^{-5}$  to  $3 \times 10^{-3}$  A. For 0.3 Torr of Ar, constrictions were observed for currents from  $1.5 \times 10^{-4}$  to  $10^{-3}$  A. For N<sub>2</sub> discharges constrictions were observed for currents between 0.3 and 2 mA at 0.3 Torr, between 0.05 and 3 mA at 1 Torr, and 0.1 and 30 mA at 0.3 Torr. At 0.3 Torr the brightness of the constricted area changed as the current changed, rather than the brightness remaining fixed as the area changed.

## SECTION VI

### SEARCH FOR ABSORPTION BY $N_2^+$

A search was made for absorption at wavelengths of lines of the Meinel band of  $N_2^+$  ions in the cathode fall of  $N_2$  discharges. The apparatus was the same as that used for our previous measurements of absorption by  $N_2^+$  in the positive column of pulsed discharges except that the diode beam was parallel to the electrodes of the discharge cell shown in Figure 1. Because of distortion of the laser beam by the quartz cylinder, only two passes of the laser beam through the cathode-fall region were possible.

Several preparatory experiments were performed using the positive column discharge described in Section II of WRDC-TR-90-2081. Attempts to obtain satisfactory absorption signal-to-noise ratios by modulating the discharge current at frequencies in the kilohertz range were unsuccessful because of very large noise components to the laser output and/or the discharge at these frequencies. Attempts to modulate the laser diode at 50 kHz were also unsuccessful because of mode hopping. The development of a double modulation scheme in which the laser is optically modulated at frequencies of  $\approx 1$  MHz and the discharge is modulated at a lower frequency was not pursued because of the equipment costs and effort that would be required.

Measurements were made of the integrated absorption cross section for the  $R_1(4)$  line of the  $A^2\Pi_u \leftarrow X^2\Sigma_g^+$  ( $v' = 2, v'' = 0$ ) band because this line is well isolated from interfering lines of the  $B^3\Pi_g \leftarrow A^3\Sigma_u$  transition. The first series of measurements were made during the afterglow of a 10  $\mu s$  discharge at peak currents from 0.4 to 1.4 A. These conditions were chosen because of the better signal-to-noise ratio resulting from the lower

interference from discharge emission and the near absence of Doppler shift in the line position. The integrated absorption was calculated from spectral scans and extrapolated to the end of the discharge using the measured time dependence of absorption at line center. The positive ion-electron density was calculated from the measured current and the previously measured electron drift velocity. The results are expressed as the integrated absorption so as to take into account changes in line width with ion drift. The integrated absorption was observed to be proportional to the current. The resultant integrated absorption cross section was  $5.5 \pm 1 \times 10^{-17} \text{ cm}^2 \text{ cm}^{-1}$  per  $\text{N}_2^+$  ion. Data were also obtained during the discharge, but have not yet been analyzed.

Assuming that the absorption linewidth and  $\text{N}_2^+$  density in the cathode fall are  $0.03 \text{ cm}^{-1}$  and  $10^{10} \text{ cm}^{-3}$ , the peak absorption coefficient is  $\approx 2 \times 10^{-5} \text{ cm}^{-1}$  for a current of  $\approx 50 \text{ mA}$ . This means a fractional absorption of  $\approx 0.02\%$  for the  $12 \text{ cm}$  path of our experiment.

## SECTION VII

### ELECTRONIC CHARGE MULTIPLICATION

The electronic charge multiplication experiments in  $N_2$  at high  $E/n$  have been discussed in detail by Gylys, Jelenković, and Phelps<sup>6</sup> for the case of a spatially uniform electric field. Here we wish to extend the technique to the spatially nonuniform electric fields characteristic of the cathode fall-negative glow regions of electrical discharges. The technique requires the release of a short pulse of photoelectrons from the cathode and the measurement of the integrated charge collected  $Q_e$  at the anode at times slightly longer than the electron transit time. This charge is proportional to the electron density weighted by the potential that the electrons traverse in the discharge. The measured charge includes the contributions of new electrons produced in the gap by electron impact ionization, although these new electrons contribute less charge per electron than those produced at the cathode because electrons produced in the gap traverse a smaller potential change. The measured charge is normalized to the charge collected when the system is evacuated  $Q_c$ .

Figure 5 shows values of  $Q_e/Q_c$  measured recently for Ar at  $E/n = 1$  kTd. The points designated by circles were obtained in the absence of a self-sustained discharge, while the squares show data obtained in the presence of self-sustained discharges from 0.5 to 5  $\mu A$ . The smooth curve is obtained by fitting the model developed for equilibrium discharges at moderate  $E/n$  discussed by Gylys et al.<sup>6</sup> The ionization coefficient given by this fit is 10% lower than published values obtained from steady-state or "Townsend" current growth experiments. We have not yet applied the nonequilibrium model of Phelps and Jelenković<sup>7</sup>

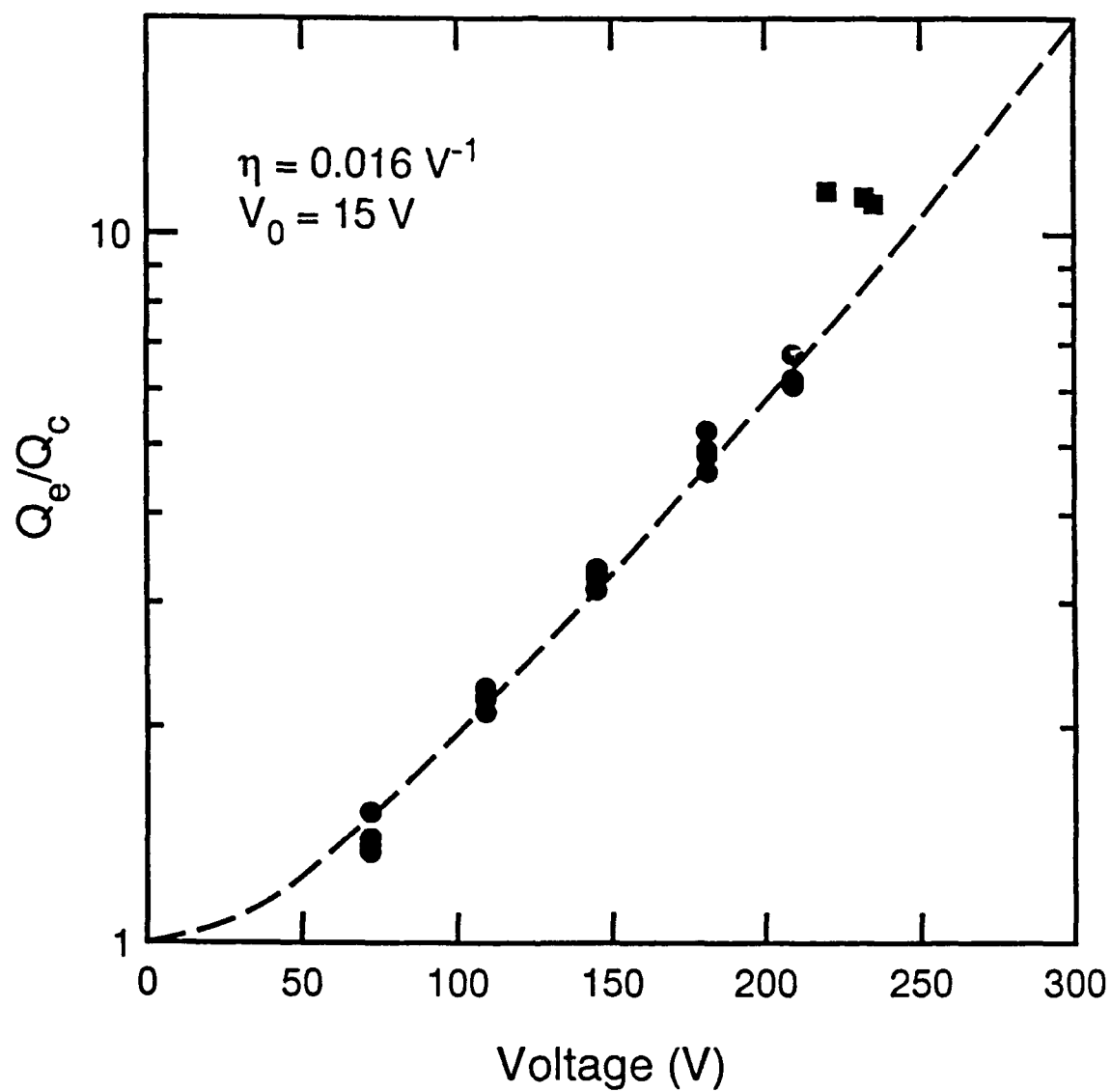


Figure 5. Electron charge ratios  $Q_e/Q_c$  for Ar at  $E/n = 1 \text{ kTd}$ .

to this situation. We do not understand the large departure from the theoretical curve for the data obtained in the presence of the self-sustained discharges, i.e., the highest voltage points shown. We suggest that this departure from the predicted extrapolation from lower voltages is the result of changes in the photoelectric yield that are caused by bombardment of the cathode by ions from the self-sustained discharge. In principle, this problem can be overcome by rapid switching of the applied voltage from the value appropriate to the self-sustained discharge to a value that is low enough such that the electron multiplication is negligible, e.g., 20 V for the conditions of Figure 5.

## SECTION VIII

### LASER-INDUCED DISCHARGE OSCILLATIONS

Measurements and analyses have been made of the current oscillations following sudden increases in current through low current, low pressure discharges in hydrogen. The currents were small enough so that the calculated space charge distortion of the electric field was small. The  $E/n$  values ranged from  $E/n$  for which the electrons are in equilibrium with the gas to  $E/n$  where nonequilibrium effects are important. The frequencies ranged from 2 to 30 kHz and the damping time constants were 100  $\mu$ s to 1 ms. These transient experiments complement the earlier ac impedance measurements for steady-state hydrogen discharges by Sigmond<sup>8</sup> at higher pressures and a lower electrode separation.

The experiments were conducted in the drift tube described in Section II, i.e., parallel plate geometry with electrodes 78 mm diameter and separated by  $d = 10$  mm. The pressures were from 0.5 to 3 Torr. The series resistance used to control the discharge current was varied from  $5 \times 10^4$  to  $5 \times 10^6$  ohms. The current was monitored with a small resistance in series with the electrode near ground potential. The discharges were visually uniform. The changes in current were produced by laser induced photoelectron pulses from the cathode. The photoelectric technique required averaging many transients to obtain a good signal to noise. The upper limit of the discharge current was determined by the onset of continuous oscillations.<sup>9</sup> The lower limit to the current was set by an overdamped approach to steady-state. Figure 6 shows representative current waveforms resulting from the short ( $\approx 10^{-8}$  s)



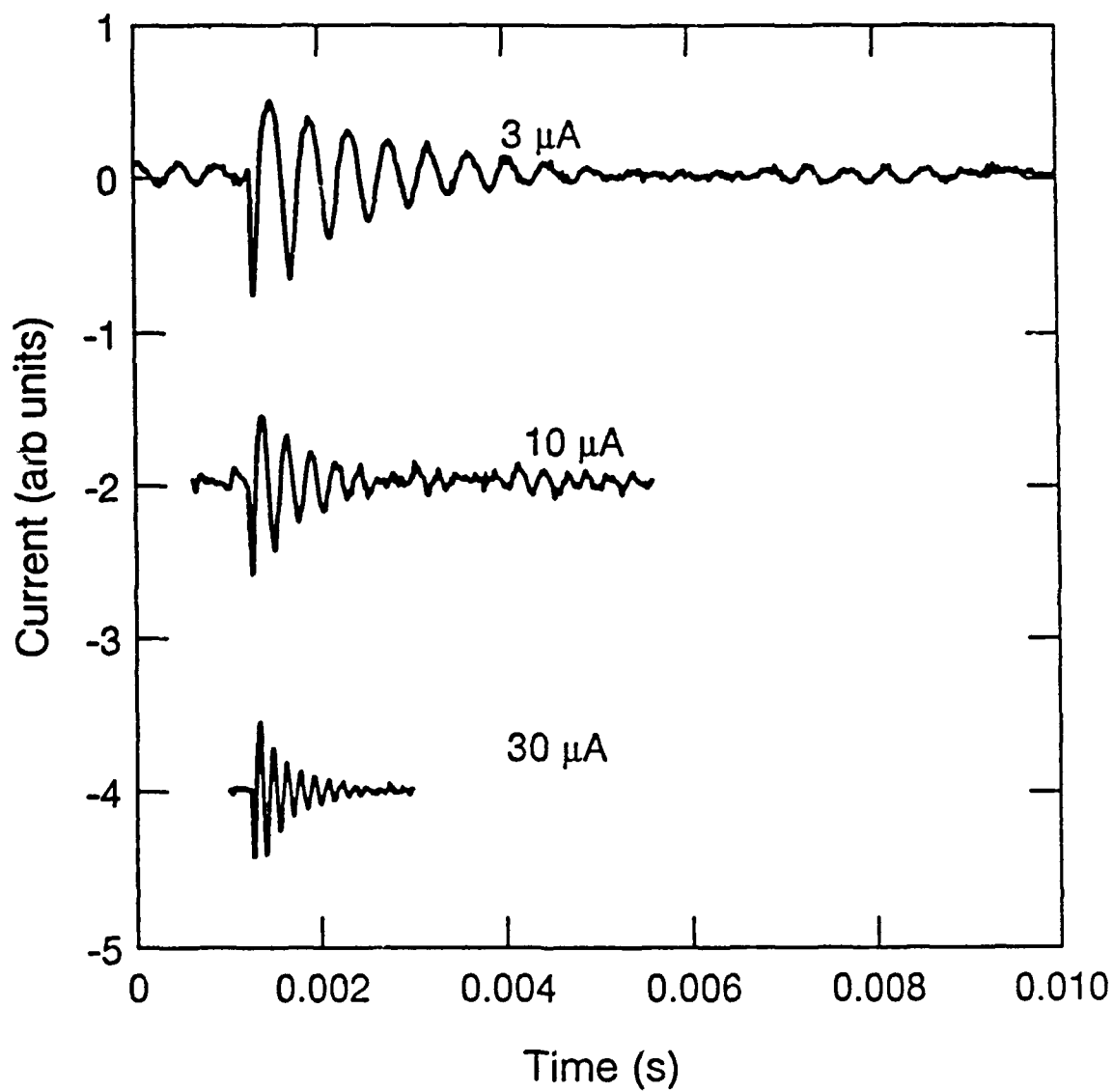


Figure 6. Photoelectron induced transient current waveforms in  $\text{H}_2$  for a  $pd = 0.5$  Torr cm.

photoelectron current pulses. The voltage waveforms show oscillations that are only a few per cent of the discharge voltage.

Measured angular frequencies  $\omega$  and damping constants  $\alpha$ , i.e., reciprocal damping time constants, are shown in Figure 7 as a function of the discharge current for a hydrogen pressure of 0.5 Torr. The dashed line shows the angular frequency variation with the square root of the current predicted using the model of discharge inductance discussed by Sigmond.<sup>8</sup> It was observed that the size of the current monitor resistor used in the experiments shown in Figure 7 was sufficient to alter the damping. Further examination of this feature is planned.

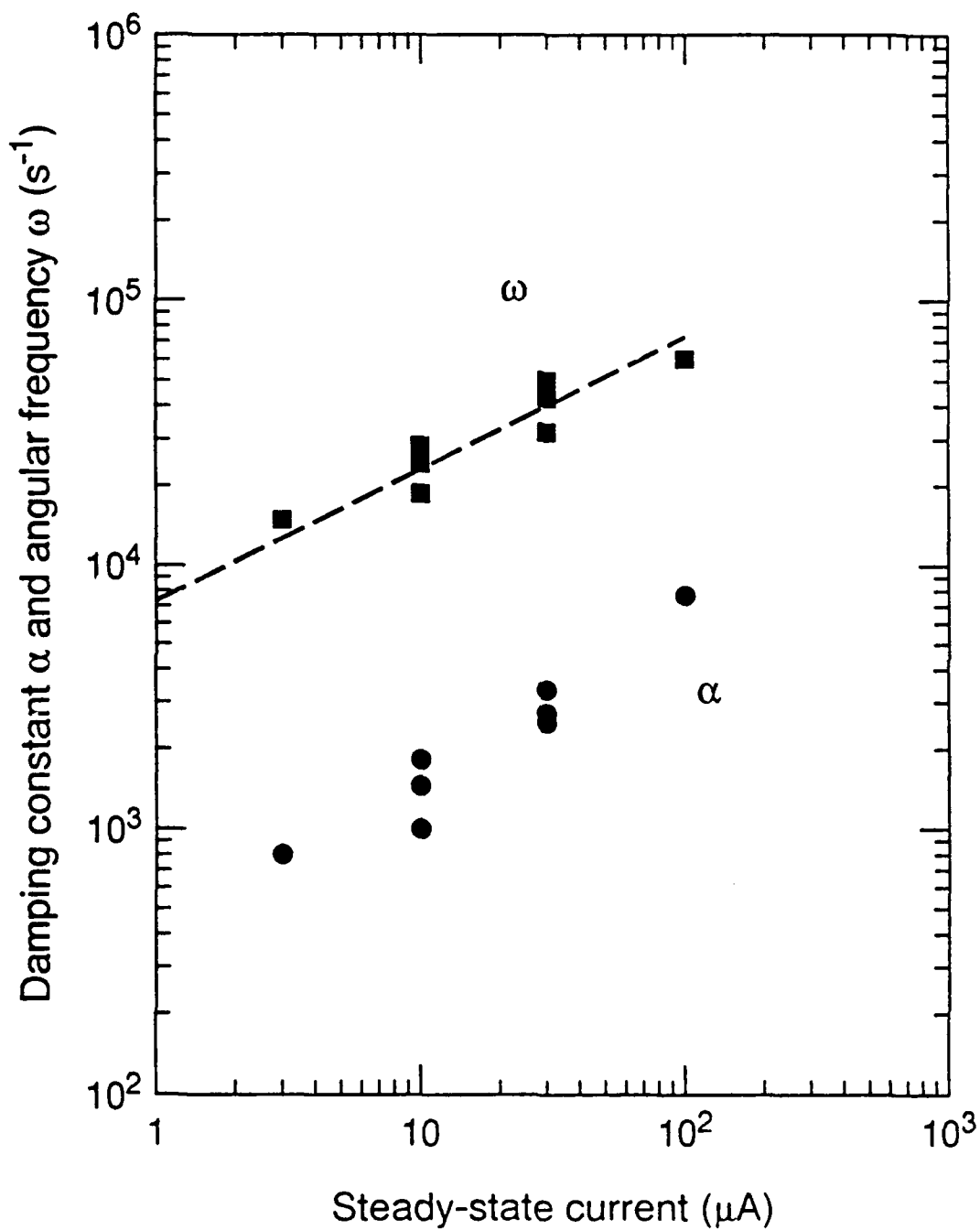


Figure 7. Angular frequency and damping constant versus current for  $\text{pd} = 0.55 \text{ Torr cm}$ .

## SECTION IX

### CONCLUSIONS AND RECOMMENDATIONS

The experiments with hydrogen discharges dominated by the cathode fall and described in this report show that a) these discharges are unstable for wide ranges of current and circuit resistance, b) increasing the circuit capacitance expanded the region of instabilities to lower currents, c) lateral constrictions of the discharge occur over a much more limited range of currents and pressures than do oscillations, d) laser-induced photoelectron pulses produce damped oscillations for a discharge currents below those at which self-sustained oscillations are observed, e) the frequency of the induced oscillations varies approximately as the square root of the discharge current, and f) the damping of the oscillations increases with discharge current in an as yet unexplained manner. Attempts to observe absorption of lines of the Meinel band by  $N_2^+$  in the cathode fall of  $N_2$  discharges were unsuccessful because of the very small anticipated signal and difficulties in properly modulating the laser diode used as a tuneable source. Measurements of the electronic charge multiplication at voltages below and above the breakdown or low-current-maintenance showed an unexpected discontinuity at the breakdown voltage. Further development of the technique will be necessary in order to obtain useful data.

We recommend that the comprehensive measurements and analyses of dc electrical discharges dominated by the cathode fall and negative glow be continued. The approaches recommended for near-term research are: a) develop and apply relationships between the measured oscillation frequency and the damping time constant of the steady-state discharge and the charge and potential distributions within the discharge to test discharge models; b)

complete the development of the electron-charge-multiplication perturbation technique; c) measure and analyze the temporal and spatial development of the cathode fall and negative glow; d) continue to look for opportunities for the development of the laser absorption technique for the measurement of  $N_2^+$  densities in  $N_2$  discharges, e.g., the availability of diode lasers operating at 391.4 nm; and e) continue the search for in situ and simple ways to characterize the secondary emission properties of "practical" cathodes. The need for such measurements and analyses is illustrated by the very large spread in the published experimental discharge voltage-current characteristics shown in our compilation.<sup>10</sup>

## REFERENCES

1. A. Guntherschulze, Z. Physik 49, 358 (1928); M. J. Druyvesteyn and F. M. Penning, Rev. Mod. Phys. 12, 87 (1940); B. N. Klyarfel'd, L. G. Guseva and A. S. Pokrovskaya-Soboleva, Zhur. Tekh. Fiz. 36, 704 (1966); [Sov. Phys. - Tech. Phys. 11, 520 (1966)].
2. K. G. Emeleus, Int. J. Electronics 42, 105 (1977).
3. See for example, G. Francis, Handb. Phys. 21, 81 (1956); J-P. Boeuf, J. Appl. Phys. 63, 1342 (1988).
4. G. L. Weissler, Handb. Phys. 21, 350 (1956).
5. B. M. Jelenković and A. V. Phelps, Phys. Rev. A 36, 5310 (1987).
6. V. T. Gylys, B. M. Jelenković, and A. V. Phelps, J. Appl. Phys. 65, 3369 (1989).
7. A. V. Phelps and B. M. Jelenković, Phys. Rev. A 38, 2975 (1988).
8. R. S. Sigmond, in Proc. 4th Int'l. Conference on Ionization Phenomena in Gases, edited by N.R. Nilsson (North-Holland, Amsterdam, 1960), p. 189.
9. Z. Lj. Petrović and A. V. Phelps, Bull. Am. Phys. Soc. 36, 200 (1991).
10. A. V. Phelps (unpublished).